Interaction of an aluminum atom with an alkaline earth atom: Spectroscopic and *ab initio* investigations of AlCa

Jane M. Behm,[a] Michael D. Morse, Alexander I. Boldyrev, and Jack Simons
Department of Chemistry, University of Utah, Salt Lake City, Utah 84112

(Received 25 March 1994; accepted 24 June 1994)

A spectroscopic analysis of diatomic AlCa generated by laser vaporization of a 2:1 Al:Ca metal alloy followed by supersonic expansion has been completed using resonant two-photon ionization spectroscopy. Four excited electronic states have been identified and investigated in the energy region from 13 500 to 17 900 cm^{-1}. These are the [13.5] $^2\Pi_r$, the [15.8] $^2\Sigma$, the [17.0] $^2\Delta_{3/2}$(?), and the [17.6] $^2\Delta_{3/2}$ states. From rotational analysis excited state bond lengths have been measured for three of the four excited states, and the ground state has been unambiguously determined as a $^2\Pi_r$ state with a weighted least squares value of the ground state bond length of $r_0'' = 3.1479 \pm 0.0010$ Å. The ionization energy of the molecule has also been directly determined as 5.072 ± 0.028 eV. *Ab initio* calculations for the potential energy curves of seven low-lying states of AlCa [$X\ ^2\Pi_r$, $^2\Sigma^+$, $^4\Sigma^-$, $^4\Pi_r$, $^2\Pi_r(2)$, $^2\Delta$, and $^2\Sigma^-$] and for the $X\ ^1\Sigma^+$ ground electronic state of $AlCa^+$ have been carried out. In agreement with experiment, $^2\Pi_r$ is calculated to be the ground electronic state of the neutral molecule. The dissociation energies of AlCa ($X\ ^2\Pi_r$) into $Al(3s^2 3p^1, {}^2P^0) + Ca(4s^2, {}^1S)$ and for $AlCa^+$ ($X\ ^1\Sigma^+$) into $Al^+(3s^2, {}^1S) + Ca(4s^2, {}^1S)$ are calculated to be 0.47 and 1.50 eV, respectively. The excited $^2\Sigma^+$, $^4\Sigma^-$, $^4\Pi_r$, $^2\Pi_r(2)$, $^2\Delta$, and $^2\Sigma^-$ states are calculated to lie 0.2, 0.7, 0.7, 1.1, 1.1, and 1.1 eV above $X\ ^2\Pi_r$, respectively, and the vertical and adiabatic ionization energies of AlCa have been calculated to be 5.03 and 4.97 eV, respectively.

I. INTRODUCTION

In this article the spectroscopic study of the transition metal aluminides initiated previously for AlCu (Ref. 1) and AlNi (Ref. 2) is continued with the investigation of AlCa, followed immediately by a study of AlZn.[3] In these investigations, we hope to probe the circumstances which dictate the preferential orientation of the lone $3p$ electron of the Al atom ($3p\sigma$ or $3p\pi$) as well as the possibility of $3p\sigma$–$3d\sigma$ and $3p\pi$–$3d\pi$ bonding in these mixed main group-transition metal molecules. Although AlCa is quite obviously not a transition metal aluminide, calcium being an alkaline earth element, it nevertheless represents a diatomic aluminide of the same period and is considered for our purposes as a transition metal without d electrons. The two transition metal aluminides previously studied, AlCu (Ref. 1) and AlNi,[2] contain transition metals which have little or no $3d \leftarrow 4s$ promotion energy. As a result a $3d^{n+1}4s^1$ configuration is readily adopted and the $4s$ electron of the transition metal can combine with the Al $3p$ electron in its $3p\sigma$ orientation to form a two electron σ^2 bond. In contrast, Ca and Zn have substantial $4p \leftarrow 4s$ promotion energies of 15 000 and 32 000 cm^{-1}, respectively.[4] Since the promotion energy is so high, the possibility of a molecular ground state deriving from an excited $4s^1 4p^1$ configuration of Ca or Zn seems rather unlikely. Instead, the ground state configuration of the AlCa or AlZn molecule will be determined by the preferential orientation of the lone Al $3p$ electron in the presence of a filled $4s^2$ configuration.

As far as we are aware, the present investigation is the only study, spectroscopic or otherwise, to have been performed on diatomic AlCa. Section II describes the experimental procedures employed to produce the AlCa molecule and record its spectrum, and in Sec. III the spectra are presented and analyzed. Section IV describes the theoretical methods used to investigate the AlCa molecule, and the results of these *ab initio* studies are presented in Sec. V, where a comparison is made to the experimental measurements. Section VI then concludes the paper with a summary of our most important findings.

II. EXPERIMENT

The resonant two-photon ionization (R2PI) apparatus employed to study diatomic AlCa has been previously described.[5] The diatomic AlCa molecule is produced by pulsed laser ablation of an approximately 2:1 molar alloy of Al:Ca in the throat of a pulsed supersonic beam of helium. The alloy was fabricated in the form of a disk, which was sanded flat and held in contact with a stainless steel block through which a pulsed supersonic flow of helium was passed. At the peak density of the helium flow, a pulsed, frequency doubled Nd:YAG laser was employed to ablate the metal atoms, which were entrained in the supersonic flow and expanded into vacuum. A previously described rotary drive mechanism[6] was employed to continuously rotate and translate the sample disk, preventing holes from being drilled into the alloy and thereby reducing the severity of the shot-to-shot fluctuations in the concentration of AlCa molecules produced in the expansion.

Two different procedures were used to prepare the metal alloy. In the first process the alloy was formed by placing the weighed component metals in a stainless steel holder in a quartz tube under vacuum, which was then heated with a Fischer burner until the metals melted and reacted exothermically to form the alloy. In the second method the weighed

[a]Kodak Fellow.

component metals were subjected to an electric arc under an argon atmosphere using an electric furnace. Both samples were similar in appearance and physical properties; they were soft and friable, easily oxidized when in contact with air for a prolonged period, and easily cracked (particularly during the cooling of the alloy from the melt). These undesirable properties were alleviated to some degree by enriching the sample in aluminum. With proper care and the use of low vaporization fluences, it was possible to maintain a fairly stable AlCa signal using this source.

Following supersonic expansion into vacuum, the molecular beam was admitted into the ionization region of a time-of-flight mass spectrometer by passage through a skimmer. There the AlCa molecules were interrogated by a Nd:YAG-pumped dye laser beam counterpropagating along the molecular beam path. For most of the experiments reported here a second, ionizing photon was supplied by a nitrogen laser (337 nm, 3.68 eV), which crossed the molecular beam at right angles. Excimer laser radiation supplied by a KrF laser (248 nm, 5.00 eV) was examined as an alternative to the nitrogen laser, but no enhanced ion signal was found, even when the dye laser was tuned to a known absorption band. On this basis it appears that AlCa is either directly ionized with one photon of KrF radiation, or KrF radiation is resonant with a transition in the molecule. In a few experiments the second, ionizing photon was generated by frequency doubling the dye laser radiation, allowing spectra to be collected in a dye+doubled dye, 1+1 REMPI process. For these experiments the second harmonic radiation was generated using an angle-tuned, servo-tracked potassium dihydrogen phosphate (KDP) crystal.

Once ionized, the molecular ions traveled up a flight tube, entered a reflectron assembly and were directed down a second flight tube to a microchannel plate detector. The resulting signal was preamplified, digitized, and processed by a DEC 11/73 microcomputer, which also controlled all of the time delays in the experiment. The optical spectra of $^{27}Al^{40}Ca$ (^{40}Ca being 97% naturally abundant) were collected by scanning the dye laser frequency while monitoring the ion signal at mass 67.

High resolution spectra were recorded by insertion of an intracavity étalon into the dye laser and pressure scanning using Freon 12 (CCl_2F_2, DuPont). The dye laser linewidth was narrowed in this manner to 0.04 cm^{-1} and absolute calibration of all of the rotationally resolved bands was obtained by comparison of a simultaneously recorded I_2 transmission spectrum with that of the I_2 atlas of Gerstenkorn and Luc[7] (within the energy range of 14 800–20 000 cm^{-1}). For the high resolution investigation of the 6-0, 7-0, and 8-0 bands of the $[13.5]\ ^2\Pi_{1/2}\leftarrow X\ ^2\Pi_{1/2}$ band system, the I_2 cell was heated to enhance the hot band absorptions present at frequencies slightly below 14 800 cm^{-1} prior to comparison with the atlas of heated I_2 absorptions.[8] Finally, in those instances where the fundamental frequency used to excite the transition under investigation was not within the range of the I_2 atlas (heated or unheated), the dye laser radiation was focused through a Raman cell filled with 500 psi of H_2. The *first* Stokes light was then used to excite the AlCa molecule and the higher frequency fundamental radiation was used for recording the I_2 transmission spectrum. A precise calibration of the spectrum was thus obtained based upon the work of Clouthier and Karolczak,[9] which demonstrates that the H_2 Raman shifting process occurs exclusively on the $Q(1)$ line, resulting in a Raman shift at 500 psi of 4155.162 cm^{-1}. Corrections were also made for the Doppler shift experienced by the molecules as they traveled toward the radiation source at the beam velocity of helium (1.77×10^5 cm/s); this correction amounted to less than 0.11 cm^{-1} for all of the bands investigated.

Excited state lifetimes were measured using the time-delayed resonant two-photon ionization method, and the exponential decay curves which were obtained were fit with a nonlinear least-squares algorithm,[10] yielding the upper state lifetimes. Deconvolution of the instrument function, which was treated as a Gaussian and allowed to vary in these fits due to the temporal instability of the N_2 laser, was included in all measurements reported here.

III. EXPERIMENTAL RESULTS

A. Low resolution spectra

Diatomic AlCa was investigated using low resolution ($\approx$0.8 cm^{-1}) resonant two-photon ionization spectroscopy in the spectral region spanning from nearly 12 800 to 20 400 cm^{-1} using fundamental dye laser radiation and from 25 650 to 36 600 cm^{-1} using frequency doubled dye laser radiation. Four recognizable band systems were observed in the region from 13 200 to 18 000 cm^{-1}, while unassigned discrete transitions were found at higher frequencies, from 18 000 to 20 400 cm^{-1}. In contrast, no spectroscopic transitions were recorded in the frequency doubled dye region from 25 650 to 36 600 cm^{-1}.

B. The $[13.5]\ ^2\Pi_r\leftarrow X\ ^2\Pi_r$ band system

Figure 1 displays the low resolution resonant two-photon ionization spectrum of the lowest frequency band system observed in diatomic $^{27}Al^{40}Ca$. The individual bands of this system are clearly red-shaded and excitation out to $v'=13$ is observed in the excited state, indicative of a significant bond lengthening upon electronic excitation. Band frequencies for the members of this and all other observed band systems are given in Table I, along with measured upper state lifetimes. Although the upper state accessed in this band system almost certainly lies above the dissociation limit to ground state atoms, and there is some variation in the lifetimes of the individual vibrational levels, this variation is too minor to indicate that predissociation plays a dominant role in the decay of the excited state. Accordingly, we consider the weighted average of the measured excited state lifetimes, 210 ns, to represent the radiative lifetime of the upper state. If the decay were dominated by fluorescence to the ground electronic state, this would correspond to an absorption oscillator strength of $f\approx0.04$, which in any case represents an upper limit.

Six members of this band system have been rotationally resolved and analyzed. The rotationally resolved spectrum of the 8-0 band displayed in Fig. 2 is typical of the results obtained. All of the rotationally resolved bands exhibit a con-

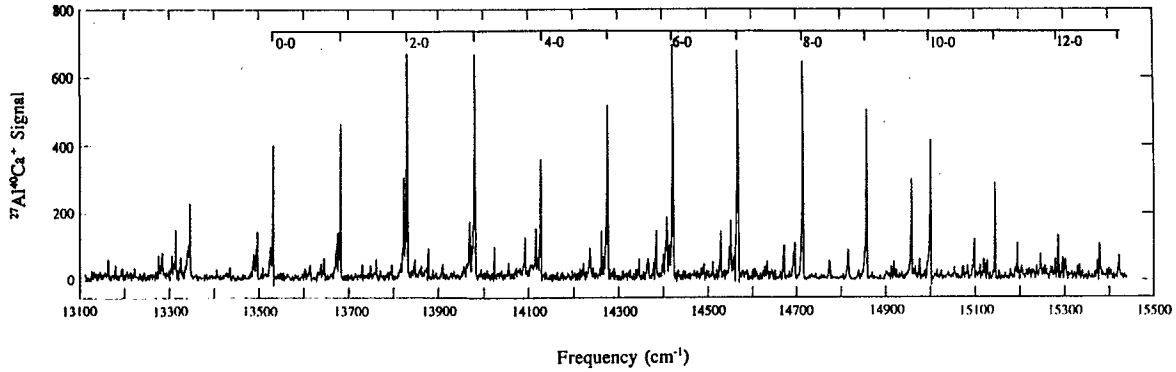

FIG. 1. Low resolution resonant two-photon ionization spectrum of the [13.5] $^2\Pi_{1/2,3/2}\leftarrow X\ ^2\Pi_{1/2,3/2}$ band system of diatomic $^{27}Al^{40}Ca$. The spectrum was collected using DCM, LDS 698, LDS 750, and LDS 751 laser dyes for excitation followed by N_2 excimer radiation for photoionization. The labeled bands correspond to the [13.5] $^2\Pi_{1/2}\leftarrow X\ ^2\Pi_{1/2}$ band system while most of the weaker bands can be assigned as either vibrational hot bands of the $\Omega'=1/2\leftarrow\Omega''=1/2$ subsystem or as bands of the [13.5] $^2\Pi_{3/2}\leftarrow X\ ^2\Pi_{3/2}$ subsystem.

spicuous bandhead in the R branch, prominent P lines, and a Q branch with intensity which rapidly diminishes with increasing J. This last feature is characteristic of parallel bands, leading us to consider assignments of 1/2←1/2, 3/2←3/2, etc., in terms of Ω. Upon detailed analysis all of the intense bands are well described as parallel bands arising from an $\Omega'=1/2\leftarrow\Omega''=1/2$ transition, supporting the assignment of the band system as $^2\Pi_{1/2}\leftarrow X\ ^2\Pi_{1/2}$. To differentiate this excited $^2\Pi$ state from other $^2\Pi$ states in this molecule, it is designated as the [13.5] $^2\Pi$ state, where [13.5] indicates the energy of the $v=0$ level of this state, relative to the $v=0$ level of the ground state, measured in thousands of wave numbers. This convention is also used to label the other observed excited states in this molecule. Measured and fitted line positions for all rotationally resolved bands of this and the remaining band systems of $^{27}Al^{40}Ca$ are available from the Physics Auxiliary Publication Service of the American Institute of Physics[11] or from the author (M.D.M.). A least squares fit of six rotationally resolved vibronic bands of the [13.5] $^2\Pi_{1/2}\leftarrow X\ ^2\Pi_{1/2}$ band system to the formula

$$\nu=\nu_0+B'J'(J'+1)-B''J''(J''+1) \tag{3.1}$$

provides the values of $B_v'([13.5]\ ^2\Pi_{1/2})$ listed in Table II, which are further analyzed to yield $B_e'([13.5]\ ^2\Pi_{1/2}) = 0.088\ 31 \pm 0.000\ 14\ cm^{-1}$, $\alpha_e'([13.5]\ ^2\Pi_{1/2}) = 0.000\ 44 \pm 0.000\ 02\ cm^{-1}$, and $r_e'([13.5]\ ^2\Pi_{1/2}) = 3.4426 \pm 0.0027$ Å. The fitted rotational constant of the ground vibronic level is obtained as a weighted average of the values from all rotationally analyzed bands as $B_0''(X\ ^2\Pi_{1/2}) = 0.105\ 45 \pm 0.000\ 07\ cm^{-1}$, which may be inverted to give $r_0''(X\ ^2\Pi_{1/2}) = 3.1504 \pm 0.0010$ Å. Correcting for spin-uncoupling effects between the $X\ ^2\Pi_{1/2}$ and $X\ ^2\Pi_{3/2}$ states using the measured separation of 65.2 cm^{-1} (see below), this provides a final estimate of the true ground state bond length of $r_0''(X\ ^2\Pi) = 3.1479 \pm 0.0010$ Å.

The low resolution spectrum shown in Fig. 1 also displays many features which are not assigned in the figure. The main progression, which is labeled, corresponds to the v'-0 bands of the [13.5] $^2\Pi_{1/2}\leftarrow X\ ^2\Pi_{1/2}$ system. An additional set of weaker features, uniformly displaced 186 cm^{-1} to the red of the main progression, corresponds to the v'-1 hot bands of the [13.5] $^2\Pi_{1/2}\leftarrow X\ ^2\Pi_{1/2}$ band system, and another set displaced 368 cm^{-1} to the red of the main progression corresponds to the v'-2 hot bands of the [13.5] $^2\Pi_{1/2}\leftarrow X\ ^2\Pi_{1/2}$ band system. A final set of vibronic features is displaced 5–25 cm^{-1} to the red of the main progression. Although these features were not rotationally resolved because of their weak intensity, they are thought to originate from the spin–orbit excited $X\ ^2\Pi_{3/2}$ state, and are assigned as v'-0 bands of the [13.5] $^2\Pi_{3/2}\leftarrow X\ ^2\Pi_{3/2}$ system. Analysis of these band positions provides spectroscopic constants of $\omega_e' = 152.2 \pm 0.1\ cm^{-1}$, $\omega_e'x_e' = 0.45 \pm 0.01\ cm^{-1}$ for the [13.5] $^2\Pi_{1/2}$ state; $\omega_e' = 150.4 \pm 0.5\ cm^{-1}$, $\omega_e'x_e' = 0.45 \pm 0.04\ cm^{-1}$ for the [13.5] $^2\Pi_{3/2}$ state; and $\omega_e'' = 189.1 \pm 0.8\ cm^{-1}$, $\omega_e''x_e'' = 1.76 \pm 0.25\ cm^{-1}$ for the $X\ ^2\Pi_{1/2}$ state.

The fact that the vibrational frequencies of the [13.5] $^2\Pi_{1/2}$ and [13.5] $^2\Pi_{3/2}$ states differ indicates that the spin–orbit constant, A, of the [13.5] $^2\Pi$ state varies with vibrational level. Presumably this occurs because the nature of the [13.5] $^2\Pi$ state is altered as the internuclear separation changes. Using the value $A_0(X\ ^2\Pi)=65.2\pm0.1\ cm^{-1}$, which is directly measured from the [15.8] $^2\Sigma\leftarrow X\ ^2\Pi_{1/2,3/2}$ band system discussed below, the vibrational dependence of $A_v([13.5]\ ^2\Pi)$ may be fit as

$$A_v([13.5]\ ^2\Pi)=(60.89\pm0.63)-(1.721\pm0.085)\times(v'+1/2)\ cm^{-1}.$$

In addition, if the two components of the [13.5] $^2\Pi$ state (and the two components of the $X\ ^2\Pi$ state) are considered together, fitted values of $T_0=13\ 524.16\pm0.36$, $\omega_e' = 151.32 \pm 0.13$, and $\omega_e'x_e' = 0.45 \pm 0.01\ cm^{-1}$ are obtained.

C. The [15.8] $^2\Sigma\leftarrow X\ ^2\Pi_{1/2,3/2}$ band system

Further to the blue in the resonant two-photon ionization spectrum of AlCa, the next band system one encounters is displayed in Fig. 3. The lower trace displays the spectrum obtained under cold conditions, while the upper trace dis-

TABLE I. Vibronic bands of $^{27}Al^{40}Ca$.

System	Band	Observed frequency (cm^{-1})[a]	Lifetime (ns)[b]	Band	Observed frequency (cm^{-1})[a]
[13.5] $^2\Pi_{1/2}$–X $^2\Pi_{1/2}$	0-0	13 527.867 3[c] (112)	282(11)	6-1	14 234.98 (−25)
	1-0	13 678.200 2[c] (18)	229(10)	7-1	14 381.61 (54)
	2-0	13 827.90 (−49)	198(30)	8-1	14 526.71 (70)
	3-0	13 977.114 2[c](−75)	277(34)	9-1	14 670.62 (58)
	4-0	14 125.80 (−63)	160 (7)	10-1	14 813.55 (38)
	5-0	14 273.77 (−31)	214(10)	11-1	14 954.08(−130)
	6-0	14 420.310 2[c](−52)	232(17)	12-1	15 096.46 (−24)
	7-0	14 566.396 4[c](−27)	242(18)	0-2	13 159.28 (22)
	8-0	14 711.576 7[c] (−3)		1-2	13 310.00 (−34)
	9-0	14 856.32 (68)		3-2	13 609.73 (−45)
	10-0	14 997.88 (−89)		4-2	13 759.05 (31)
	11-0	15 141.31 (32)		5-2	13 906.61 (21)
	12-0	15 284.04 (174)		6-2	14 053.94 (80)
	13-0	15 422.55 (−16)		8-2	14 345.33 (141)
	0-1	13 341.14 (−1)		9-2	14 487.30 (−66)
	1-1	13 492.53 (11)		10-2	14 630.38 (−70)
	2-1	13 642.19 (−60)		11-2	14 773.75 (44)
	3-1	13 792.31 (4)		12-2	14 913.38(−124)
	5-1	14 088.54 (6)			
[13.5] $^2\Pi_{1/2}$←X $^2\Pi_{3/2}$	0-0	13 521.81 (21)		6-0	14 405.19 (−12)
	1-0	13 671.75 (60)		7-0	14 549.97 (54)
	2-0	13 819.44 (−34)		8-0	14 693.28 (62)
	3-0	13 966.73 (−79)		9-0	14 837.19 (221)
	4-0	14 113.96 (−39)		10-0	14 973.23(−316)
	5-0	14 260.13 (−15)		11-0	15 117.66 (76)
[15.8] $^2\Sigma$←X $^2\Pi_{1/2}$	0-0	15 838.608 7[c](−11)	193(19)	3-3	15 963.21 (37)
	1-1	15 884.18 (137)		4-4	15 999.10 (30)
	2-2	15 925.41 (123)			
[15.8] $^2\Sigma$←X $^2\Pi_{3/2}$	0-0	15 773.381 8[c](−14)		2-2	15 857.90(−108)
	1-1	15 816.70 (−91)		3-3	15 896.62(−102)
[17.0] $^2\Delta_{3/2}$(?)	0-0	16 995.64[c] (−84)	24 (3)	0-1	16 812.50 (75)
←X $^2\Pi_{1/2}$	1-0	17 140.10[c] (27)	21 (1)	2-1	17 099.91 (99)
	2-0	17 282.38 (−127)	26 (4)	3-1	17 241.46(−174)
	3-0	17 429.76 (183)	31 (2)		
[17.0] $^2\Delta_{5/2}$(?)	0-0	16 970.33 (−4)		2-0	17 259.25 (−11)
←X $^2\Pi_{3/2}$	1-0	17 114.90 (11)		3-0	17 404.06 (4)
[17.6] $^2\Delta_{3/2}$←X $^2\Pi_{1/2}$	0-0	17 578.876 5[c]	334(37)		
	1-0	17 752.07	302(24)		
	2-0	17 922.22	414(21)		

[a]Measured vibronic band positions were fitted to the formula $\nu = T_0 + \omega'_e v' - \omega'_e x'_e(v'^2 + v') - \omega''_e v'' + \omega''_e x''_e(v''^2 + v'')$, providing the values of ω'_e, $\omega'_e x'_e$, ω''_e and $\omega''_e x''_e$ listed in Table III. Residuals ($\nu - \nu_{calc}$) are provided in units of 0.01 cm^{-1} in parentheses following each entry.

[b]Errors reported for excited state lifetimes correspond to 1σ in the nonlinear least squares fit.

[c]Measured in high resolution using the I_2 atlas for calibration.

plays a spectrum recorded using a higher vaporization fluence, resulting in a vibrationally hotter spectrum. Under cold conditions the spectrum is dominated by a single band, with a weaker secondary feature some 65 cm^{-1} to the red. No higher vibrational members of a v'-0 progression are observed, suggesting that Franck–Condon factors place nearly all of the intensity of the system in the 0-0 vibrational band. Under warmer conditions additional features are observed which are assigned as members of a $\Delta v = 0$ sequence. These are associated with both peaks found in the colder spectrum, and the similarity in measured intervals suggests that the two features observed in the colder spectrum derive from the same electronic transition, but differ in the spin-orbit components which are involved.

Figure 4 displays a rotationally resolved scan over the intense 0-0 feature located at 15 839 cm^{-1}. The spectrum is nearly symmetrical, fanning out to both the blue and the red from an obvious band origin. Nevertheless, the spectrum is quite dense, suggesting a [15.8] $^2\Sigma$←X $^2\Pi_{1/2}$ assignment. Assuming negligible spin doubling in the $^2\Sigma$ state and unobservably small lambda doubling in the X $^2\Pi_{1/2}$ state, such a transition would lead to four branches, labeled as P_{11},

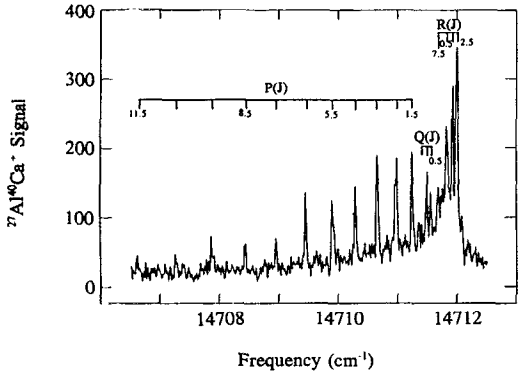

FIG. 2. High resolution scan revealing the rotational structure of the 8-0 band of the $[13.5]\ ^2\Pi_{1/2}\leftarrow X\ ^2\Pi_{1/2}$ band system. Similar rotational scans were collected for the 0-0, 1-0, 3-0, 6-0, and 7-0 bands, providing a value of $B'_e = 0.088\ 31 \pm 0.000\ 14\ cm^{-1}$ which converts to an equilibrium excited state bond length of $r'_e = 3.443 \pm 0.003$ Å.

$Q_{11}+P_{21}$, $R_{11}+Q_{21}$, and R_{21}. Moreover, if the rotational constants of the upper and lower states were identical (as is very close to the case here), the standard formulas[12] would predict rotational branches as

$$\begin{aligned} P_{11}(J'') &= \nu_0 + B'(J''-3/2)(J''-1/2) - B''J''(J''+1) \\ &\approx \nu_0 - 3BJ'' + 3B/4, \\ Q_{11}+P_{21}(J'') &= \nu_0 + B'(J''-1/2)(J''+1/2) \\ &\quad - B''J''(J''+1) \\ &\approx \nu_0 - BJ'' - B/4, \\ R_{11}+Q_{21}(J'') &= \nu_0 + B'(J''+1/2)(J''+3/2) \\ &\quad - B''J''(J''+1) \\ &\approx \nu_0 + BJ'' + 3B/4, \\ R_{21}(J'') &= \nu_0 + B'(J''+3/2)(J''+5/2) - B''J''(J''+1) \\ &\approx \nu_0 + 3BJ'' + 15B/4. \end{aligned} \tag{3.2}$$

Thus, one would expect a pair of inside branches, with lines spaced by B (the $Q_{11}+P_{21}$ and $R_{11}+Q_{21}$ branches) along with a pair of outside branches, with lines spaced by $3B$ (the P_{11} and R_{21} branches). These expectations are in close accord with the spectrum of Fig. 4, and a fit of the observed

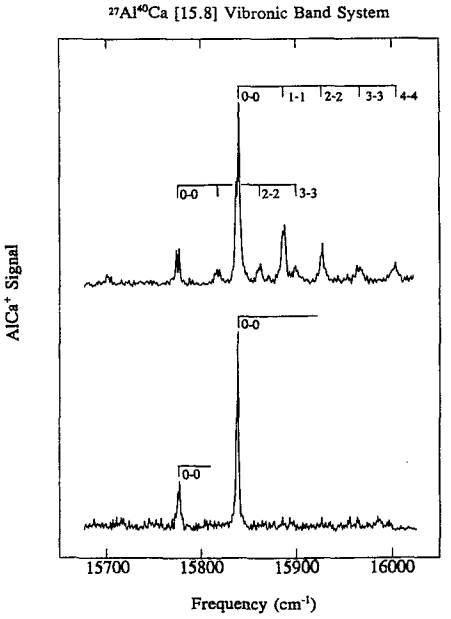

FIG. 3. Low resolution spectrum of the $[15.8]\ ^2\Sigma\leftarrow X\ ^2\Pi_{1/2,3/2}$ band system. The lower spectrum was collected employing a rhodamine 640/DCM 1:1 dye laser mix for excitation in conjunction with the doubled dye light for photoionization, as described in the text. In the upper panel the ionization photon was supplied by a N_2 excimer laser, but more importantly, an increase in laser vaporization fluence was utilized to populate vibrational and spin-orbit excited states, resulting in the observation of numerous hot bands. It is this upper spectrum, combined with the knowledge of the ground state vibrational frequency (from the $[13.5]\ ^2\Pi_r\leftarrow X\ ^2\Pi_r$ band system) that permits an estimate of the vibrational frequency for the $[15.8]\ ^2\Sigma$ excited state of $\omega'_e = 235.9 \pm 1.1\ cm^{-1}$.

rotational transitions to the exact formulae (setting the spin–rotation constant of the upper $^2\Sigma$ state, γ', and the Λ-doubling constant of the lower state, q'', equal to zero) results in an excellent fit, providing $B''_0 = 0.104\ 74 \pm 0.000\ 19\ cm^{-1}$ and $B'_0 = 0.103\ 74 \pm 0.000\ 16\ cm^{-1}$. This fitted value of $B''_0(X\ ^2\Pi_{1/2})$ is close to the weighted average of $0.105\ 45 \pm 0.000\ 07\ cm^{-1}$, and the value of $B'_0([15.8]\ ^2\Sigma)$ may be inverted to provide a $v=0$ bond length of $r'_0([15.8]\ ^2\Sigma) = 3.176 \pm 0.002$ Å. The close similarity between this bond length and that of the $X\ ^2\Pi$ state (3.1479 ± 0.0010 Å, when corrected for spin-uncoupling effects) explains the lack of bands with $\Delta v \neq 0$ in the low resolution spectrum.

TABLE II. Fitted constants for rotationally analyzed bands of $^{27}Al^{40}Ca$.[a]

System	Band	ν_0 (cm^{-1})	B''_0 (cm^{-1})	B'_v (cm^{-1})
$[13.5]\ ^2\Pi_{1/2}\leftarrow X\ ^2\Pi_{1/2}$	0-0	13 527.867 3 (28)	0.105 63 (14)	0.088 17 (14)
	1-0	13 678.200 2 (31)	0.105 16 (31)	0.087 13 (40)
	3-0	13 977.114 2 (21)	0.105 85 (25)	0.087 10 (31)
	6-0	14 420.310 2 (27)	0.104 93 (30)	0.084 53 (37)
	7-0	14 566.396 4 (33)	0.104 95 (22)	0.084 32 (26)
	8-0	14 711.576 7 (21)	0.105 96 (13)	0.084 91 (15)
$[15.8]\ ^2\Sigma\leftarrow X\ ^2\Pi_{1/2}$	0-0	15 838.608 7 (34)	0.104 74 (19)	0.103 74 (16)
$[17.6]\ ^2\Delta_{3/2}\leftarrow X\ ^2\Pi_{1/2}$	0-0	17 578.876 5 (30)	0.105 24 (17)	0.096 30 (17)

[a]All values are reported in wave numbers (cm^{-1}), with 1σ error limits given in parentheses.

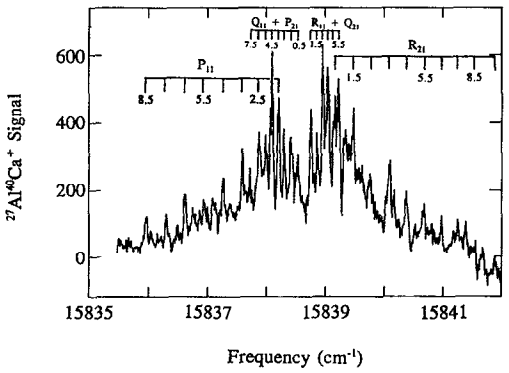

FIG. 4. Rotationally resolved scan of the 0-0 band of the [15.8] $^2\Sigma \leftarrow X\ ^2\Pi_{1/2}$ band system. The similar ground and excited state bond lengths allow the presence of four branches to be readily evident (the spin–rotation and Λ-doubling constants being negligible) and a fit of the rotational lines then provides the [15.8] $^2\Sigma$ bond length of $r_0' = 3.176 \pm 0.002$ Å.

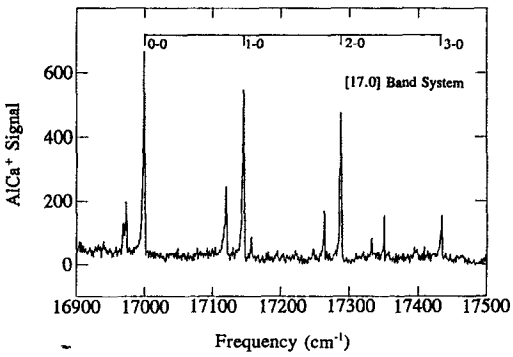

FIG. 5. Low resolution spectrum of the [17.0] $^2\Delta_{3/2,5/2}(?) \leftarrow X\ ^2\Pi_{1/2,3/2}$ band system of $^{27}Al^{40}Ca$, recorded using rhodamine 640, 610, and 590 to provide the first photon in the resonant two-photon ionization process. The second, ionizing photon is provided by the second harmonic of the dye laser radiation.

Returning to the low resolution spectrum, the band located at 15 773.4 cm^{-1} which is evident in the colder spectrum is assigned as the 0-0 band of the [15.8] $^2\Sigma \leftarrow X\ ^2\Pi_{3/2}$ system, originating from the spin–orbit excited $\Omega''=3/2$ level of the ground $X\ ^2\Pi$ state. Because both this band and the intense 0-0 band of the [15.8] $^2\Sigma \leftarrow X\ ^2\Pi_{1/2}$ system at 15 838.61 cm^{-1} terminate on the same upper state, they may be used to determine the spin–orbit splitting in the ground $X\ ^2\Pi$ state. Although a lack of intensity prevented a rotational analysis of the 0-0 band of the [15.8] $^2\Sigma \leftarrow X\ ^2\Pi_{3/2}$ system, a high resolution scan over this feature, recorded simultaneously with the transmission spectrum of I_2, provided an accurate measurement of the band origin. Combining this with the fitted band origin of the 0-0 band of the [15.8] $^2\Sigma \leftarrow X\ ^2\Pi_{1/2}$ system then provides $A_{v=0}(X\ ^2\Pi) = 65.2 \pm 0.1$ cm^{-1}. This value is slightly reduced from the spin–orbit constant of atomic aluminum in its $3s^2 3p^1$, $^2P^0$ ground state [$\zeta_{3p}(Al) = 74.7$ cm^{-1}],[13] and is somewhat reduced from the values measured for the $X\ ^2\Pi$ ground states of AlAr [where values of 80.9 ± 2 (Ref. 14) and 79.8 ± 5 cm^{-1} (Ref. 15) have been reported] and AlKr [where values of 78.4 ± 4 (Ref. 14) and 78.4 ± 5 cm^{-1} (Ref. 15) have been reported]. The reduction in spin–orbit splitting in AlCa as compared to $\zeta_{3p}(Al)$ suggests that the unpaired π electron in AlCa may not reside totally in an unperturbed $3p\pi$ orbital on aluminum, and suggests a stronger chemical interaction in AlCa as compared to AlAr and AlKr.

The hot band intervals measured from the upper spectrum of Fig. 3 may be combined with the vibrational constants of the ground state, determined from the analysis of the [13.5] $^2\Pi \leftarrow X\ ^2\Pi$ system, to obtain the vibrational constants of the [15.8] $^2\Sigma$ state. This leads to values of $\omega_e' = 235.9 \pm 1.1$ cm^{-1} and $\omega_e' x_e' = 3.1 \pm 0.2$ cm^{-1} for the [15.8] $^2\Sigma$ state of AlCa.

In addition to these results, the excited state lifetime of the $v=0$ level of the [15.8] $^2\Sigma$ state was measured, yielding a value of $\tau = 193 \pm 19$ ns. If the [15.8] $^2\Sigma$ state decays entirely by fluorescence to the ground $X\ ^2\Pi$ electronic state, this corresponds to an absorption oscillator strength of $f \approx 0.03$. In any case this represents an upper limit to the absorption oscillator strength.

D. The [17.0] $^2\Delta_{3/2,5/2}(?) \leftarrow X\ ^2\Pi_{1/2,3/2}$ band system

Continuing to the blue in the resonant two-photon ionization spectrum of AlCa, the next band system that is encountered is displayed in Fig. 5. The spectrum is dominated by a progression of four strong bands, which are accompanied by weaker features lying 25 cm^{-1} to the red. In addition, a series of vibrational hot bands, displaced 186 cm^{-1} to the red of the main progression, grows in under hot conditions (not displayed in Fig. 5). A vibronic fit of the main progression along with its hot bands provides vibrational constants of $\omega_e' = 142.9 \pm 2.9$ cm^{-1}, $\omega_e' x_e' = -0.2 \pm 0.7$ cm^{-1}, and $\Delta G_{1/2}'' = 184.7 \pm 1.4$ cm^{-1}. The ground state vibrational interval obtained from this band system, $\Delta G_{1/2}''$, is in excellent agreement with the value of $\Delta G_{1/2}'' = 185.6 \pm 0.9$ cm^{-1} obtained from the analysis of the [13.5] $^2\Pi_r \leftarrow X\ ^2\Pi_r$ band system.

Attempts to rotationally resolve the bands of this system were for the most part unsuccessful. Nevertheless, a head was evident in the R branch, and the pattern of intensity in the branches seemed to indicate a $\Delta\Omega = +1$ transition, with R more intense than Q, which in turn was more intense than P. Under high resolution the bands appeared rather similar to those of the [17.6] $^2\Delta_{3/2} \leftarrow X\ ^2\Pi_{1/2}$ system described below, suggesting a possible $^2\Delta$ upper state for the [17.0] $\leftarrow X\ ^2\Pi$ system, which may be tentatively assigned as the [17.0] $^2\Delta(?) \leftarrow X\ ^2\Pi$ system.

The main features of the system are assigned as originating from the ground spin–orbit level and are designated as the [17.0] $^2\Delta_{3/2}(?) \leftarrow X\ ^2\Pi_{1/2}$ system. Weaker vibronic features, lying 25 cm^{-1} to the red of the main features of the spectrum, are assigned as the [17.0] $^2\Delta_{5/2}(?) \leftarrow X\ ^2\Pi_{3/2}$ subbands. The $^2\Delta_{5/2}(?)$ upper state of these subbands has similar vibrational constants as the $^2\Delta_{3/2}(?)$ state, with $\omega_e' = 144.3 \pm 0.3$ cm^{-1} and $\omega_e' x_e' = -0.06 \pm 0.08$ cm^{-1}. Given that the spin–orbit splitting of the ground state has now been directly measured as 65.2 ± 0.1 cm^{-1}, the spin–

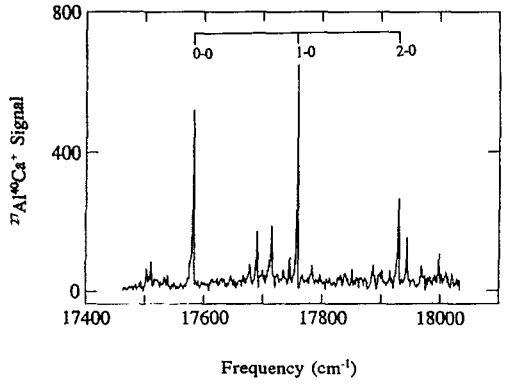

FIG. 6. Low resolution spectrum of the [17.6] $^2\Delta_{3/2,5/2}\leftarrow X\ ^2\Pi_{1/2,3/2}$ band system of $^{27}Al^{40}Ca$, obtained using rhodamine 590 to provide the first photon in the resonant two-photon ionization process. The second, ionizing photon is supplied by an excimer laser operating on the N_2 transition at 3371 Å.

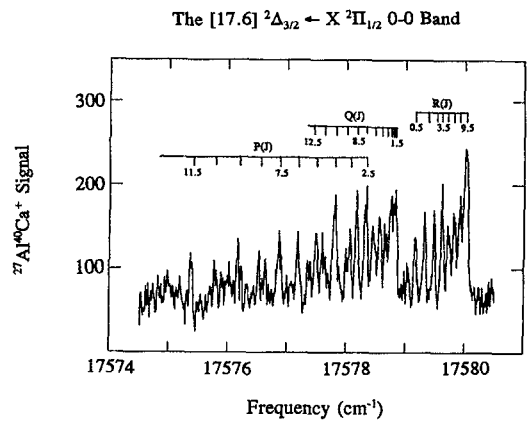

FIG. 7. High resolution scan over the 0-0 band of the [17.6] $\Omega'=3/2\leftarrow X\ ^2\Pi_{1/2}$ band system. The bandhead which gradually forms in the R branch indicates a lengthening of the bond upon electronic excitation, confirmed by the rotational fit which yields an excited state bond length of $r_0' = 3.295 \pm 0.003$ Å.

orbit splitting of the [17.0] $^2\Delta(?)$ state is determined to be 39.1 ± 1.4 cm^{-1}, which results in a spin–orbit constant of $A=19.6\pm0.7$ cm^{-1}.

Decay lifetimes of several vibrational levels of the [17.0] $^2\Delta(?)$ state have been measured, as indicated in Table I. No significant dependence on the vibrational quantum number is evident, suggesting that predissociation is not contributing strongly to the decay mechanism. A weighted least-squares average of the measured values results in a value of $\tau=22\pm1$ ns. If the excited [17.0] $^2\Delta(?)$ state decays entirely by fluorescence to the ground state, this corresponds to an absorption oscillator strength of $f\approx0.2$. In any case this value provides an upper limit on the absorption oscillator strength of the [17.0] $^2\Delta(?)\leftarrow X\ ^2\Pi$ system.

E. The [17.6] $^2\Delta_{3/2}\leftarrow X\ ^2\Pi_{1/2}$ band system

Slightly to the blue of the [17.0] $^2\Delta_{3/2,5/2}(?)\leftarrow X\ ^2\Pi_{1/2,3/2}$ band system lies another short vibronic progression which can be tentatively designated the [17.6] $^2\Delta_{3/2}\leftarrow X\ ^2\Pi_{1/2}$ system. As shown in Fig. 6, only three vibrational quanta are observed, yielding a vibrational frequency of $\omega_e' = 171.7 \pm 0.9$ cm^{-1}. The lifetime of this excited electronic state is measured as $\tau=361\pm15$ ns, establishing without doubt that the upper state of this system is different from the [17.0] $^2\Delta(?)$ state. The $\Omega'=5/2\leftarrow\Omega''=3/2$ component of the [17.6] $^2\Delta_{3/2,5/2}\leftarrow X\ ^2\Pi_{1/2,3/2}$ band system was not observed in these studies. A rotationally resolved spectrum of the presumed 0-0 band (in the absence of isotopic shift information this assignment is not conclusive) is displayed in Fig. 7. In contrast to the bands of the [17.0] state the R lines are well-resolved, although the Q and especially the P lines suffer from a similar lack of intensity. A fit of the measured line positions to Eq. (3.1) yields values of $B_0'' = 0.105\ 24 \pm 0.000\ 17$ cm^{-1} and $B_0' = 0.096\ 30 \pm 0.000\ 17$ cm^{-1}, consistent with a bond lengthening from 3.148 ± 0.001 Å (determined from a weighted average of all determinations of the ground state rotational constant, corrected for the effects of spin-uncoupling) to 3.295 ± 0.003 Å upon electronic excitation. A summary of all of the theoretically predicted (see below) and spectroscopically analyzed states of AlCa is provided in Table III.

F. Ionization energy of AlCa

In addition to allowing one to mass-selectivity probe the spectroscopy of species produced in a laser ablation experiment, the resonant two-photon ionization method provides a convenient means of measuring the ionization energy of the molecule under study. In the present case of AlCa, spectroscopic features observed using a dye+doubled-dye, 1+1 REMPI process could not be observed using KrF radiation (248 nm, 5.00 eV) as the second, ionizing photon. This observation suggested that KrF radiation either ionizes the AlCa molecule directly in a one-photon process, or is resonant with a molecular transition. A more definite result was obtained by operating the excimer laser on the N_2 transition (337 nm, 3.68 eV) and rescanning the transitions that were discovered in the dye+doubled-dye 1+1 REMPI process. When this experiment was performed, new transitions were discovered at lower frequencies than could be detected using the dye+doubled dye method. In particular, the 0-0 and 0-1 bands of the [13.5] $^2\Pi_{1/2}\leftarrow X\ ^2\Pi_{1/2}$ system were found to be unobservable using the dye+doubled-dye scheme, but were readily apparent using the nitrogen laser for the photoionization step. Our inability to observe these bands in the dye +doubled-dye scheme is probably due to an inadequate amount of energy for the ionization step. Including a correction for the field ionization shift of the ionization energy, the lowest frequency band observed by the dye+doubled-dye method provides an upper limit on the ionization energy of AlCa of IE(AlCa)$\leqslant$5.100 eV, while the highest frequency band which is unobservable by this method provides a lower limit of IE(AlCa)$\geqslant$5.044 eV. These may be combined to provide IE(AlCa)$=5.072\pm0.028$ eV.

It is puzzling that the ionization energy deduced in this experiment is slightly above the energy of the KrF excimer

TABLE III. Electronic states of $^{27}Al^{40}Ca$.[a]

State	T_0 (cm^{-1})[b]	ω_e (cm^{-1})	$\omega_e x_e$ (cm^{-1})	B_e (cm^{-1})	α_e (cm^{-1})	r_e (Å)	τ (ns)	μ (D)[h]
[17.6] $^2\Delta_{3/2}$	17 578.876 5	176.23	1.52	B_0=0.096 30 (7)		3.295 (3)[c]	361 (15)	
[17.0] $^2\Delta_{5/2}$(?)	17 035.53	144.3 (3)	−0.06 (8)					
[17.0] $^2\Delta_{3/2}$(?)	16 995.64	142.9 (29)	−0.2 (7)				22 (1)	
[15.8] $^2\Sigma$	15 838.608 7	235.9 (11)	3.1 (2)	B_0=0.103 74(16)		3.176 (2)[d]	193 (19)	
[13.5] $^2\Pi_{3/2}$	13 587.0	150.4 (5)	0.45 (4)					
[13.5] $^2\Pi_{1/2}$	13 527.867 3	152.2 (1)	0.45 (1)	0.088 31(14)	0.000 44 (2)	3.4426(27)[e]	210	
$^2\Sigma^-$ [f]	9 248[f]	195[f]				3.045[f]		4.2
$^2\Delta$[f]	9 242[f]	231[f]				2.916[f]		3.2
$^2\Pi(2)$[f]	8 788[f]	177[f]				3.317[f]		3.4
$^4\Pi$[f]	6 056[f]	206[f]				3.179[f]		3.2
$^4\Sigma^-$ [f]	5 932[f]	301[f]				2.912[f]		4.7
$^2\Sigma^+$ [f]	1 796[f]	124[f]				3.622[f]		−0.6
$X\ ^2\Pi_{3/2}$	65.2(1)					3.1479(10)[g]		3.1
$X\ ^2\Pi_{1/2}$	0	189.1 (10)	1.76(32)	B_0=0.105 45 (7)				

[a]1σ error limits for fitted parameters are provided in parentheses, in units of the last digit quoted for the parameter.
[b]Energies are measured from the $v=0$ level of the $X\ ^2\Pi_{1/2}$ state to the $v=0$ level of the state in question.
[c]This is the value of r_0 calculated from B_0 for this spin–orbit level, and has not been corrected for spin-uncoupling perturbations by the other spin–orbit level of this state.
[d]This is r_0, not r_e.
[e]This is r_e, but the value has not been corrected for spin-uncoupling perturbations.
[f]Calculated as described in the text at the CASSCF-MRCISD(Q) level.
[g]This is r_0 for the $X\ ^2\Pi$ ground state, and has been corrected for the effects of spin-uncoupling.
[h]Calculated at the CASSCF-MRCISD level.

laser radiation (248 nm, 4.997 eV), yet resonant enhancement could not be obtained using KrF radiation for photoionization. A likely explanation for this phenomenon is that the KrF laser radiation may be resonant with one of the many Rydberg levels which are present in diatomic AlCa as one approaches the ionization limit. Theoretical work reported below provides a slightly lower value of 4.97 eV for the ionization energy of AlCa, but computational methods frequently underestimate ionization energies because the correlation energy is typically more accurately calculated in the cation than in the neutral. In addition, the experimental results are extremely reproducible and highly convincing in favor of the 5.072±0.028 eV value.

IV. THEORETICAL METHODS

Two theoretical tools were used for calculations of the low-lying electronic states of AlCa and for the ground state of the $AlCa^+$ cation. Because both theoretical methods are nonrelativistic, we were not able to calculate spin–orbit splittings for comparison to experimental measurements; the determination of these parameters is beyond the accuracy of our calculations.

A. MRCISD calculations

In the first method, the complete active space (CAS) self-consistent field (SCF) method was used to generate a basis of dominant electronic configurations for further multireference all single- and double-excitation configuration interaction calculations (CASSCF-MRCISD).[16] The final CASSCF-MRCISD energies were corrected using the Davidson method[17] [CASSCF-MRCISD(Q)] to account for quadruple and higher order excited configurations. For these calculations, we used large atomic natural orbital (ANO) basis sets which for Al consisted of $(17s12p5d4f)$ elementary functions and $[7s5p3d2f]$ contracted functions,[18] and for the Ca atom of $(15s13p4d)$ elementary and $[9s7p2d]$ contracted functions.[19] The orbital active space included $4a_1$, $2b_1$, $2b_2$, and $1a_2$ type orbitals (C_{2v} symmetry labeled). All 5 valence electrons were considered as active in the CASSCF calculations.

With this number of active electrons and orbitals, we obtain 470 configurations for $^2\Pi$ electronic states, 484 configurations for $^2\Sigma^+$ states, 264 configurations for $^4\Sigma^-$ states, 252 configurations for $^4\Pi$ states, and 466 configurations for $^2\Delta$ and $^2\Sigma^-$ states to use in CASSCF expansions of the respective reference wave functions. All of these functions were then used in subsequent MRCISD calculations in which the total number of configurations were 345 602 for $^2\Pi$ states, 347 048 for $^2\Sigma^+$ states, 245 280 for $^4\Sigma^-$ states, 246 908 for $^4\Pi$ states, and 344 310 for $^2\Delta$ and $^2\Sigma^-$ states. The first and second excited states of a given symmetry were calculated as the second and third roots of the secular equation in the MRCISD calculations.

The $AlCa^+$ cation was studied with the same atomic basis sets and using an active orbital space for CASSCF calculations of $5a_1$, $2b_1$, $2b_2$, and $1a_2$ orbitals. This leads to 233 configurations in the CASSCF expansion of the reference wave function and gives 64 560 final configurations in the MRCISD expansion. The MRCISD potential energy data points were fit to an analytical form using cubic spline interpolation, after which the rovibrational Schrödinger equation was solved numerically (using Numerov's method) for one vibrational state at a time and for three rotational quantum numbers. All of these electronic and rovibrational calculations were performed using the MOLCAS-2 computer program.[20] In addition, excitation and ionization energies of the Al and Ca atoms were calculated to test the accuracy of the approach. The calculated values of IE(Al)=5.98 eV,

TABLE IV. Calculated electronic states of AlCa.

Method		$X^2\Pi$	$^2\Sigma^+$	$^4\Sigma^-$	$^4\Pi$	$^2\Pi(2)$	$^2\Delta$	$^2\Sigma^-$	$^1\Sigma^+$ [a]
QCISD(T)									
r_e (Å)		3.213	3.572	2.857					3.510
E (total) (a.u.)		−918.716 73	−918.708 52	−918.694 07					−918.536 49
T_e (cm^{-1})		0	1802	4973					39 558
CASSCF-MRCISD									
r_e (Å)		3.277	3.653	2.928	3.176	3.194	2.908	2.963	3.531
ω_e (cm^{-1})		172	118	230	207	193	238	233	158
E (total) (a.u.)		−918.726 78	−918.718 01	−918.699 90	−918.700 07	−918.680 70	−918.684 70	−918.675 93	−918.546 29
T_e (cm^{-1})		0	1925	5899	5862	10 114	9235	11 160	39 615
μ(Debye)[b]		3.1[b]	−0.6[b]	4.7[b]	3.2[b]	3.4[b]	3.2[b]	4.2[b]	
CASSCF-MRCISD(Q)									
r_e (Å)		3.268	3.622	2.912	3.179	3.317	2.916	3.045	3.533
ω_e (cm^{-1})		169	124	301	206	177	231	195	156
E (total) (a.u.)		−918.729 06	−918.720 77	−918.702 33	−918.701 55	−918.689 03	−918.687 09	−918.686 98	−918.546 57
T_e (cm^{-1})		0	1819	5866	6038	8784	9211	9235	40 051
Gross atomic populations[c]									
Al	$1s$	5.94	5.90	5.87	5.91	5.93	5.90	5.89	5.97
	$2p_0$	2.62	3.09	2.34	2.91	2.90	2.15	2.20	2.86
	$2p_{1+}$	2.87	2.06	2.80	2.83	2.74	2.89	2.78	2.05
	$2p_{1-}$	2.05	2.06	2.80	2.05	2.05	2.89	2.78	2.05
	$3d_0$	0.04	0.04	0.02	0.03	0.03	0.00	0.02	0.01
	$3d_{1+}$	0.04	0.02	0.06	0.06	0.05	0.05	0.05	0.01
	$3d_{1-}$	0.01	0.02	0.06	0.01	0.01	0.05	0.05	0.00
	$3d_{2+}$	0.01	0.00	0.01	0.01	0.01	0.02	0.02	0.00
	$3d_{2-}$	0.01	0.00	0.01	0.01	0.01	0.02	0.02	0.00
Ca	$1s$	7.18	7.56	6.75	6.73	6.73	6.70	6.75	6.96
	$2p_0$	4.07	4.21	4.06	4.30	4.29	4.18	4.10	3.98
	$2p_{1+}$	4.08	4.05	4.13	4.10	4.19	4.03	4.15	4.01
	$2p_{1-}$	4.03	4.05	4.13	4.00	4.00	4.03	4.15	4.01
	$3d_0$	0.01	0.01	0.01	0.01	0.01	0.01	0.01	0.00
	$3d_{1+}$	0.02	0.00	0.02	0.02	0.03	0.03	0.02	0.00
	$3d_{1-}$	0.00	0.00	0.02	0.00	0.00	0.03	0.02	0.00
	$3d_{2+}$	0.00	0.00	0.00	0.00	0.00	0.00	0.00	0.00
	$3d_{2-}$	0.00	0.00	0.00	0.00	0.00	0.00	0.00	0.00
Q (Al)[d]		−0.62	−0.19	−0.88	−0.84	−0.74	−0.99	−0.81	−0.03

[a]The $^1\Sigma^+$ state calculated here is the ground state of $AlCa^+$.
[b]As defined in this article, $\mu>0$ corresponds to a charge distribution in the sense Al^-Ca^+.
[c]Gross atomic populations are obtained from the CASSCF-MRCISD calculation, with $1s$ representing the sum of all s electrons on a center, $2p_0$ representing the sum of all $p\sigma$ electrons on a center, etc.
[d]Q (Al) represents the Mulliken atomic charge on aluminum.

IE(Ca)=5.88 eV, Ca $^3P^0 \leftarrow {}^1S$ excitation energy (1.68 eV), and Ca $^1P^0 \leftarrow {}^1S$ excitation energy (3.03 eV) agree with the experimental values of 5.98, 6.11, 1.89, and 2.93 eV,[4] respectively, to an accuracy of ≈0.2 eV.

B. QCISD(T) calculations

In the second theoretical approach, the QCISD(T) method[21] was used for geometry optimization using large atomic orbital basis sets. For the Al atom, the basis consists of $(17s12p2d1f)$ elementary functions and $[10s7p2d1f]$ contracted functions, and for the Ca atom $(14s11p7d2f)$ elementary and $[8s7p6d2f]$ contracted functions. The Al basis set was constructed from the basis of Shaefer *et al.* $(17s12p)$ (Ref. 22) by contracting into $[10s7p]$ according to a (6,3,1,1,1,1,1,1,1,1;6,1,1,1,1,1,1) scheme. Subsequently $2d$ and $1f$ elementary functions, taken from the GAUSSIAN-92 basis library, were added.[23] The Ca basis set was built from that of Shaefer *et al.* $(14s11p)$ (Ref. 22) by contraction to $[8s7p]$, following which $7d$ and $2f$ elementary functions contracted to $6d$ and $2f$ functions were added, as recommended by Bauschlicher *et al.*[24] All core orbitals were kept frozen in the QCISD(T) calculations. These calculations were performed using the GAUSSIAN-92 program.[23]

The calculated ionization energies of aluminum (5.93 eV) and calcium (5.89 eV), and the Ca $^3P^0 \leftarrow {}^1S$ excitation energy (1.67 eV) again agree with the corresponding experimental values of 5.98, 6.11, and 1.89 eV,[4] respectively to ≈0.2 eV. This level of agreement serves as a test of the quality of the calculations for the AlCa and $AlCa^+$ molecules. In addition, because these atomic test calculations give virtually the same results using either the MRCISD or the QCISD(T) methods, we feel comfortable in proceeding to use both approaches for the AlCa and $AlCa^+$ molecules. Comparisons of the results of various levels of calculation are presented in Table IV.

V. THEORETICAL RESULTS AND COMPARISON WITH EXPERIMENT

A. Molecular orbitals of AlCa

Although the molecular orbitals of AlCa certainly vary a bit with the state under consideration, it is useful to describe their predominant character before describing the nature of the ground and excited states. The lowest valence 1σ molecular orbital is mainly the $3s$ atomic orbital of the aluminum atom (which makes a contribution of 0.97 to this MO in the $X\ ^2\Pi$ ground state). It is therefore mainly nonbonding in character. The 2σ molecular orbital is composed of $3s_{\mathrm{Al}}$, $3p_{z,\mathrm{Al}}$, and $4s_{\mathrm{Ca}}$, with bonding interactions between $3p_{z,\mathrm{Al}}$ and $4s_{\mathrm{Ca}}$ and antibonding interactions between $3s_{\mathrm{Al}}$ and $4s_{\mathrm{Ca}}$. At long range this orbital is bonding in character, but antibonding interactions become more important at short range, causing occupation of this orbital to increase the bond length of the molecule. The 3σ orbital is antibonding with respect to the $3p_{z,\mathrm{Al}}-4s_{\mathrm{Ca}}$ interaction, but bonding with respect to the $3p_{z,\mathrm{Al}}-4p_{z,\mathrm{Ca}}$ interaction. The 1π molecular orbital is primarily $3p\pi_{\mathrm{Al}}$ in character, with a small contribution from $3d\pi_{\mathrm{Al}}$ and $4p\pi_{\mathrm{Ca}}$, and is slightly bonding in character.

Occupation of the 2σ orbital leads to a transfer of electrons from the $4s_{\mathrm{Ca}}$ orbital into the $3p_{z,\mathrm{Al}}$ orbital, leading to a substantial $\mathrm{Al}^-\mathrm{Ca}^+$ ionic character in many of the states of AlCa. This charge transfer from calcium to aluminum is largely responsible for the bonding in the molecule.

B. $^2\Pi$ states of AlCa

The interaction of ground state $\mathrm{Al}(3s^2 3p^1, {}^2P^0_{1/2,3/2})$ and $\mathrm{Ca}(4s^2, {}^1S_0)$ yields only two Hund's case (a) states, a $^2\Sigma^+$ state and a $^2\Pi$ state. The orientation of the Al $3p$ electron ($p\sigma$ or $p\pi$) thus dictates the state symmetry. In the present study the ground state of AlCa is determined both experimentally and theoretically to be a $^2\Pi_r$ state corresponding to $p\pi$ orientation of the Al $3p$ electron. Experimental molecular parameters of $r_0=3.1479\pm0.0010$ Å, $\omega_e=189.1\pm0.8$ cm^{-1}, $\omega_e x_e=1.76\pm0.25$ cm^{-1}, and spin–orbit constant $A=65.2\pm0.1$ cm^{-1} have been determined for this state. If one assumes that the ground state potential is well-described by a Morse potential, an approximate bond energy of $D_e=5079\pm723$ cm^{-1} (0.63 ± 0.09 eV) is obtained through the relation $D_e=\omega_e^2/4\omega_e x_e$, with the suggested error limit obtained simply by propagation of the errors in ω_e and $\omega_e x_e$. This is much larger than the bond energies of van der Waals molecules such as AlAr [$D_0^0(\mathrm{AlAr})=0.0152\pm0.0005$ eV] (Ref. 14) and AlKr [$D_0^0(\mathrm{AlKr})=0.0241\pm0.0001$ eV],[14] suggesting rather strongly that there is a significant chemical interaction between aluminum and calcium in the diatomic AlCa molecule.

The present gas phase analysis has unambiguously determined that the ground states of AlCa and AlZn (as is presented in the following paper)[3] are $X\ ^2\Pi_{1/2}$. The bond lengths of AlCa (3.1479 ± 0.0010 Å) and AlZn (2.6957 ± 0.0004 Å) (Ref. 3) are rather long in comparison to the bond lengths of AlCu (2.3389 ± 0.0004 Å) (Ref. 1) and AlNi (2.3211 ± 0.0007 Å).[2] Although the dissociation energies of AlCa and AlZn are poorly known, it appears that they are rather small as compared to the bond strengths of AlCu (2.315 ± 0.012 eV) (Ref. 1) and AlNi (2.29 ± 0.05 eV).[2] Both properties indicate that the bonding in AlCa and AlZn is of a very different nature and much weaker than the bonding in either AlNi or AlCu.

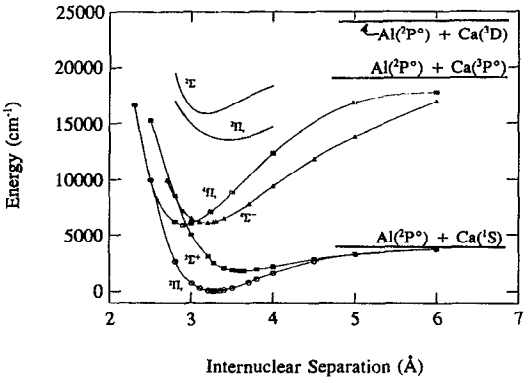

FIG. 8. Potential energy curves for the AlCa molecule. The low energy $^2\Pi_r$, $^2\Sigma^+$, $^4\Sigma^-$, and $^4\Pi_r$ potential curves are calculated results obtained at the CASSCF-MRCISD(Q) level, while the higher energy [13.5] $^2\Pi_r$ and [15.8] $^2\Sigma$ curves are derived from our spectroscopic experiments.

Our calculated potential energy curves for the lowest four electronic states of AlCa are shown in Fig. 8 along with experimentally determined potential curves for the higher energy electronic states. The experimental curves are plotted as Morse potentials using the experimental values of r_e, ω_e, and $\omega_e x_e$ (for the [13.5] $^2\Pi_r$ state) and r_0, ω_e, and $\omega_e x_e$ (for the [15.8] $^2\Sigma$ state). The corresponding molecular constants are presented in Table III and a comparison of results calculated at different levels of theory is provided in Table IV. In agreement with experiment, the ground state is calculated to be of $^2\Pi_r$ symmetry, with a $1\sigma^2 2\sigma^2 1\pi^1$ dominant electronic configuration ($C=+0.8853$). Among the 345 602 configuration state functions (CSFs) used to describe $^2\Pi$ states, only one other configuration has a CI expansion amplitude larger than 0.2: $1\sigma^2 2\sigma^0 3\sigma^2 1\pi^1$ (-0.2547). The effect of this secondary configuration may be seen in the natural occupation numbers of the lowest valence molecular orbitals, which are $1\sigma^{1.89}2\sigma^{1.73}3\sigma^{0.20}4\sigma^{0.02}5\sigma^{0.01}1\pi_x^{0.96}1\pi_y^{0.05}2\pi_x^{0.04}2\pi_y^{0.03}3\pi_x^{0.01}3\pi_y^{0.01}$.

This ground electronic state correlates with the ground atomic states of $\mathrm{Al}(3s^2 3p^1, {}^2P^0)$ and $\mathrm{Ca}(4s^2, {}^1S)$. The charge distribution in the ground $X\ ^2\Pi_r$ state has strong ionic character, with Mulliken atomic charges of $\mathrm{Al}^{-0.62}\mathrm{Ca}^{+0.62}$ and a dipole moment of $\mu=3.1$ D obtained from our MRCISD wave function. The AlCa ($X\ ^2\Pi_r$) state is weakly bound with $D_e=0.47$–0.49 eV at all levels of theory, and is very flat with a harmonic frequency of 168 cm^{-1}, which is slightly smaller than the experimental value of 189 cm^{-1}. As a result of the flatness of the potential, the predicted equilibrium bond length is very sensitive to the level of theory and varies from 3.21 Å at the QCISD(T) level to 3.27 Å at the CASSCF-MRCISD(Q) level (see Table IV), both of which are longer than the experimental value of r_0'' $= 3.1479 \pm 0.0010$ Å.

The first excited state of $^2\Pi$ symmetry, $^2\Pi_r(2)$, again has one dominant electronic configuration in the MRCISD ex-

pansion, in this case $1\sigma^2 2\sigma^{\alpha} 1\pi^{\beta} 3\sigma^{\alpha}$ ($C=0.8654$), and arises from the $X\ ^2\Pi_r$ ground state by promotion of an electron from the 2σ into the 3σ molecular orbital. This is clearly seen in the natural orbital occupation numbers of the lowest valence MOs of this state, $1\sigma^{1.89} 2\sigma^{1.05} 3\sigma^{0.89} 4\sigma^{0.03} 5\sigma^{0.02} 1\pi_x^{0.90} 1\pi_y^{0.05} 2\pi_x^{0.09} 2\pi_y^{0.02} 3\pi_x^{0.01} 3\pi_y^{0.01}$. This $^2\Pi$ electronic state correlates with $Al(^2P^0)+Ca(^3P^0)$ and also has ionic character with natural atomic charges of $Al^{-0.74}Ca^{+0.74}$ and $\mu=3.4$ D obtained from the MRCISD wave function. According to our best calculations, the vertical excitation energy $[^2\Pi_r(2)\leftarrow X\ ^2\Pi_r]$ is 1.09 eV (8800 cm^{-1}) and the adiabatic excitation energy, $T_e[^2\Pi_r(2)\leftarrow X\ ^2\Pi_r]$, is 1.09 eV (8784 cm^{-1}), both evaluated at the CASSCF-MRCISD(Q) level of theory. This is much lower in energy than the experimentally observed [13.5] $^2\Pi_r\leftarrow X\ ^2\Pi_r$ band system, and indicates that the $^2\Pi_r(2)$ state calculated in the present study does not correspond to the [13.5] $^2\Pi_r$ state that is experimentally observed.

Unfortunately, the quality of our calculation for the third root of $^2\Pi$ symmetry, $^2\Pi(3)$, is not high. This is evident because the Davidson correction for this state is quite large {−0.065 692 a.u. [at R(Al–Ca)=3.270 Å] compared to −0.002 275 a.u. and −0.008 456 a.u. for the $X\ ^2\Pi_r$ and $^2\Pi_r(2)$ states, respectively}. A large Davidson's correction implies a large contribution from quadruple and higher excitations, further implying that our CASSCF initial basis set is incapable of accurately describing this state. Therefore the geometry of this $^2\Pi(3)$ state was not optimized. As a rough estimate, however, we have calculated the $^2\Pi(3)\leftarrow X\ ^2\Pi_r$ excitation energy at the CASSCF-MRCISD level. This vertical excitation energy is approximately 21 000 cm^{-1}. The large negative Davidson's correction found for this state, however, implies that when a much larger CASSCF-CI calculation is performed the predicted energy of the state will be much lower, consistent with the observed [13.5] $^2\Pi_r$ state located near 13 500 cm^{-1}. Accordingly, we assign the [13.5] $^2\Pi_r$ state as the third state of $^2\Pi$ symmetry in the AlCa molecule. At the present level of theory, we find that this state is not well-represented by a single configuration, with 10 configurations having CI coefficients greater than 0.1 and 5 having coefficients greater than 0.2. The multiconfigurational nature of this state, which probably varies significantly with internuclear separation, may well account for the strong dependence of the observed spin–orbit splitting of the [13.5] $^2\Pi_r$ state on the vibrational quantum number, v.

C. $^2\Sigma^+$ states of AlCa

The lowest $^2\Sigma^+$ state of AlCa has a $1\sigma^2 2\sigma^2 3\sigma^1$ dominant electronic configuration ($C=0.9016$) in the MRCISD expansion and is the first excited state of the molecule. From the total of 347 048 CSFs, only three other configurations have coefficients larger than 0.1. These are $1\sigma^2 2\sigma^{\alpha} 3\sigma^{\beta} 4\sigma^{\alpha}$ (−0.1514), $1\sigma^2 2\sigma^0 3\sigma^1 1\pi_x^2$ (0.1048), and $1\sigma^2 2\sigma^0 3\sigma^1 1\pi_y^2$ (0.1048). (These last two contributions must be equal to insure a $^1\Sigma^+$ coupling of the two π electrons.) The natural occupation numbers of the lowest valence MOs are $1\sigma^{1.89} 2\sigma^{1.81} 3\sigma^{0.96} 4\sigma^{0.05} 5\sigma^{0.01} 1\pi_x^{0.06} 1\pi_y^{0.06} 2\pi_x^{0.04} 2\pi_y^{0.04} 3\pi_x^{0.02} 3\pi_y^{0.02}$, showing the dominance of the Hartree–Fock configuration in the multiconfigurational wave function. This electronic state also correlates with the ground electronic states of $Al(^2P^0)$ and $Ca(^1S)$ (see Fig. 8), and represents the $p\sigma$ approach of aluminum to the calcium atom.

The vertical $^2\Sigma^+\leftarrow X\ ^2\Pi_r$ excitation energy is computed to be 0.31 eV and the adiabatic excitation energy, $T_e(^2\Sigma^+\leftarrow X\ ^2\Pi_r)$, is 0.23 eV. The $^2\Sigma^+$ state has a much more covalent character than the $X\ ^2\Pi_r$ ground state, with Mulliken atomic charges of $Al^{-0.19}Ca^{+0.19}$ and $\mu=-0.6$ D obtained from the MRCISD wave function. Because the 3σ molecular orbital is antibonding and the 1π orbital is bonding, electron transfer from 1π into 3σ during the $^2\Sigma^+\leftarrow X\ ^2\Pi_r$ excitation leads to an increase in the equilibrium bond length of 0.35 Å. The potential energy curve of the $^2\Sigma^+$ state is even flatter than that of the ground state and has a calculated harmonic frequency of only $\omega_e=124$ cm^{-1}.

The [15.8] $^2\Sigma\leftarrow X\ ^2\Pi_r$ band system experimentally observed at 15 839 cm^{-1} certainly does not correspond to the lowest $^2\Sigma^+\leftarrow X\ ^2\Pi_r$ transition according to our calculations, which predict the lowest $^2\Sigma^+$ state to lie only 1800 cm^{-1} above the $X\ ^2\Pi_r$ state. The observed [15.8] $^2\Sigma$ state therefore corresponds to either a higher root of $^2\Sigma^+$ symmetry or to a $^2\Sigma^-$ state.

D. $^4\Sigma^-$ states of AlCa

The lowest $^4\Sigma^-$ state has a $1\sigma^2 2\sigma^1 1\pi_x^1 1\pi_y^1$ dominant electronic configuration ($C=0.9288$) in the MRCISD expansion and is the second excited state of AlCa (see Fig. 8). Only the configuration $1\sigma^0 2\sigma^1 3\sigma^2 1\pi_x^1 1\pi_y^1$ has an expansion coefficient (0.1099) larger than 0.1 from among all 245 280 CSFs in the MRCISD expansion. The natural occupation numbers of the lowest valence MOs in this state are $1\sigma^{1.88} 2\sigma^{0.97} 3\sigma^{0.07} 4\sigma^{0.02} 5\sigma^{0.01} 1\pi_x^{0.96} 1\pi_y^{0.96} 2\pi_x^{0.03} 2\pi_y^{0.03} 3\pi_x^{0.01} 3\pi_y^{0.01}$, showing the dominant contribution of the Hartree–Fock configuration to the wave function.

This $^4\Sigma^-$ electronic state correlates with the $Al(^2P^0)+Ca(^3P^0)$ excited separated atom limit (see Fig. 8). The vertical $^4\Sigma^-\leftarrow X\ ^2\Pi_r$ excitation energy is predicted to be 0.89 eV and the adiabatic excitation energy, $T_e(^4\Sigma^-\leftarrow X\ ^2\Pi_r)$, is 0.73 eV. The $^4\Sigma^-$ state is calculated to have strong ionic character with Mulliken atomic charges of $Al^{-0.88}Ca^{+0.88}$ and $\mu=4.7$ D obtained from the MRCISD wave function. Because the 2σ orbital favors large internuclear separations and the 1π orbital favors small internuclear separations, electron transfer from 2σ into 1π during the $^4\Sigma^-\leftarrow X\ ^2\Pi_r$ excitation leads to a significant decrease in the equilibrium bond length of 0.36 Å.

The *second* excited state of $^4\Sigma^-$ symmetry, $^4\Sigma^-(2)$, calculated as the second root of the secular problem, cannot be represented by a single configuration. Ten CSFs have expansion coefficients larger than 0.1 and four have coefficients larger than 0.2. The configurations making the greatest contributions to the $^4\Sigma^-(2)$ state are $1\sigma^1 2\sigma^2 1\pi_x^1 1\pi_y^1$(+0.5279), $1\sigma^2 2\sigma^0 3\sigma^1 1\pi_x^1 1\pi_y^1$ (−0.4725), $1\sigma^{\alpha} 2\sigma^{\beta} 3\sigma^{\alpha} 1\pi_x^{\alpha} 1\pi_y^{\alpha}$ (−0.3874), and $1\sigma^{\alpha} 2\sigma^{\alpha} 3\sigma^{\beta} 1\pi_x^{\alpha} 1\pi_y^{\alpha}$ (−0.2184). This leads to natural occupation numbers of the lowest valence MOs of $1\sigma^{1.49} 2\sigma^{0.97} 3\sigma^{0.46} 4\sigma^{0.02} 5\sigma^{0.01} 1\pi_x^{0.92} 1\pi_y^{0.92} 2\pi_x^{0.07} 2\pi_y^{0.07} 3\pi_x^{0.01} 3\pi_y^{0.01}$. The vertical excitation energy $[^4\Sigma^-(2)\leftarrow X^2\Pi_r]$ is 2.8 eV (22 490 cm^{-1}) and has a moderate contribution from the Davidson correction (−0.007 59 a.u.).

Because this state cannot readily be experimentally observed, due to spin selection rules, further calculations of its full potential energy curve were not pursued.

E. $^4\Pi$ states of AlCa

The lowest $^4\Pi_r$ state of AlCa has a $1\sigma^2 2\sigma^1 1\pi_x^1 3\sigma^1$ dominant configuration ($C=0.9439$) in the MRCISD expansion and is the third excited state of AlCa (see Fig. 8). All other configurations have coefficients less than 0.1. The natural orbital occupation numbers of the lowest valence molecular orbitals in this state are $1\sigma^{1.89} 2\sigma^{0.99} 3\sigma^{0.97} 4\sigma^{0.02} 5\sigma^{0.01} 1\pi_x^{0.97} 1\pi_y^{0.05} 2\pi_x^{0.03} 2\pi_y^{0.01} 3\pi_x^{0.01} 3\pi_y^{0.00}$, showing the dominant contribution of the Hartree–Fock configuration to the wave function.

This $^4\Pi_r$ state correlates with the Al $(3s^2 3p^1, {}^2P^0)$+Ca$(4s^1 4p^1, {}^3P^0)$ excited separated atom limit, as shown in Fig. 8. The vertical $^4\Pi_r \leftarrow X\ ^2\Pi_r$ excitation energy is predicted to be 0.76 eV and the adiabatic excitation energy, $T_e(^4\Pi_r \leftarrow X\ ^2\Pi_r)$, is 0.75 eV. The $^4\Pi_r$ state is calculated to have strong ionic character with Mulliken atomic charges of $Al^{-0.84}Ca^{+0.84}$ and $\mu=3.2$ D obtained from the MRCISD wave function. In comparing the $^4\Pi_r$ and the $^4\Sigma^-$ states one finds that the movement of an electron from the 1π orbital (which favors short bond lengths) in the $^4\Sigma^-$ state to the 3σ orbital (which favors long bond lengths) in the $^4\Pi_r$ state results in an elongation of the bond length from 2.912 to 3.179 Å and a reduction in the calculated vibrational frequency from 301 to 206 cm^{-1}. Nevertheless, both the $^4\Pi_r$ and the $^4\Sigma^-$ states lie at similar energies above the $X\ ^2\Pi$ state.

F. $^2\Delta$ and $^2\Sigma^-$ states of AlCa

The lowest $^2\Delta$ and $^2\Sigma^-$ states of AlCa have two dominant electronic configurations in the MRCISD expansion; $1\sigma^2 2\sigma^\alpha 1\pi_x^\beta 1\pi_y^\alpha$ (with $C=+0.64$ for the $^2\Delta$ state and $C=+0.60$ for the $^2\Sigma^-$ state) and $1\sigma^2 2\sigma^\alpha 1\pi_x^\alpha 1\pi_y^\beta$ ($C=-0.64$ for the $^2\Delta$ state and $C=+0.60$ for the $^2\Sigma^-$ state). All other CSF's have CI coefficients less than 0.2. Note that the $^2\Delta$ and $^2\Sigma^-$ states do not truly have major contributions from two distinct configurations; the two configurations listed here must be combined with coefficients that have equal absolute magnitudes to generate states of Σ^- and Δ symmetry. Therefore, our need to use two CSF's to generate these functions is purely an artifact resulting from our choice of working with the $1\pi_x$, $1\pi_y$ orbitals rather than the $1\pi_{+1}$, $1\pi_{-1}$ angular momentum eigenfunctions.

These two states have been calculated as the first and second roots of the MRCISD equations in C_{2v} symmetry. The Davidson's correction is found to be small for the first root (the $^2\Delta$ state) but is relatively large for the second root (the $^2\Sigma^-$ state). However, both states are nearly degenerate at the CASSCF-MRCISD(Q) level. As a result, the quality of our calculations for these two states may not be high, so the calculated molecular properties should only be considered as rough estimates for these states. They have ionic character with natural atomic charges of $Al^{-0.99}Ca^{+0.99}$ ($^2\Delta$ state) and $Al^{-0.81}Ca^{+0.81}$ ($^2\Sigma^-$ state) and dipole moments of 3.2 ($^2\Delta$ state) and 4.2 D ($^2\Sigma^-$ state). The vertical excitation energies for both states from the $X\ ^2\Pi_r$ ground state are approximately 1.3 eV or 9500 cm^{-1}, and the adiabatic excitation energies are approximately 1.2 eV or 9000 cm^{-1} at the CASSCF-MRCISD(Q) level.

The experimentally observed $^2\Delta$ states lie more than 17 000 cm^{-1} above the $X\ ^2\Pi_r$ ground state, again implying that the experimentally observed states are not the lowest states of $^2\Delta$ symmetry. Unfortunately, we were not able to calculate the higher roots of the secular equation in $^2\Delta$ symmetry at a reasonable level of accuracy, so we are not able to make a comparison to these experimental results.

G. The $X\ ^1\Sigma^+$ state of $AlCa^+$ and the ionization energy of AlCa

The $1\sigma^2 2\sigma^2$, $^1\Sigma^+$ electronic state of $AlCa^+$, which correlates to the $Al^+(^1S)$+Ca(^1S) separated atom limit, is expected to be the ground electronic state of the cation. The $1\sigma^2 2\sigma^2$ CSF was found to be the dominant electronic configuration ($C=0.9111$) in the MRCISD expansion, and the natural orbital occupation numbers of the lowest valence MOs were found to be $1\sigma^{1.89} 2\sigma^{1.77} 3\sigma^{0.20} 4\sigma^{0.01} 5\sigma^{0.01} 1\pi_x^{0.05} 1\pi_y^{0.05} 2\pi_x^{0.01} 2\pi_y^{0.01}$, showing the dominant contribution of the Hartree–Fock configuration to the multiconfigurational wave function. The vertical and adiabatic ionization energies of AlCa are predicted to be 5.03 and 4.97 eV, respectively, which are in reasonable agreement with the experimental value of IE(AlCa)=5.072±0.028 eV. The bond length in $AlCa^+$ is approximately 0.3 Å longer than in the $X\ ^2\Pi_r$ ground state of AlCa, because an electron is removed from the bonding 1π orbital. Despite this increase in bond length, $AlCa^+$ is more strongly bound than the neutral AlCa molecule, with $D_e(Al^+-Ca)$ calculated to be 1.50 eV using both computational methods. The bond length of $AlCa^+(X\ ^1\Sigma^+)$ was calculated to be 3.510 Å at the QCISD(T) level and 3.533 Å at the CASSCF-MRCISD(Q) level.

As shown in Table IV, the Mulliken atomic charge on aluminum in the $AlCa^+$ cation is -0.03, demonstrating that the ground state of the $AlCa^+$ ion has an electronic parentage of $Al+Ca^+$. At first glance this might be somewhat surprising, given that the ionization energies of the atoms are very similar (and that aluminum actually has a slightly lower ionization potential). On the other hand, combination of an aluminum atom in its $3p\sigma$ orientation with a calcium cation (with its $4s^1$, ^2S ground term) can result in the formation of a full covalent bond through the $3p\sigma_{Al}$–$4s\sigma_{Ca}$ interaction, this dominates the bonding in $AlCa^+$. Alternatively, if one considers the system to derive from the Al^+, $3s^2 3p^0$, ^1S+Ca $4s^2$, ^1S limit, the empty $3p\sigma$ orbital of aluminum is ideally set up to receive electrons from calcium via a dative interaction, and if one considers the two σ electrons involved in this interaction to be shared equally between the two centers, then one full electron is effectively transferred to aluminum, again leading to atomic charges of roughly zero on aluminum and +1 on calcium. As in most of the low-lying states of the neutral molecule, the direction of electron donation is from calcium to aluminum. This results not from the superior electron donating ability of calcium (a question-

able premise), but from the presence of a good acceptor orbital on the aluminum atom.

VI. CONCLUSION

Unlike the previously studied AlCu (Ref. 1) and AlNi (Ref. 2) molecules, which are characterized by a $p\sigma$ approach of an aluminum atom to a $3d^n4s^1$ transition metal atom, the present investigation shows the bonding in the ground state of AlCa to derive from a $p\pi$ approach of the aluminum atom to the stable $3d^04s^2$ configuration of calcium. A similar $p\pi$ approach of aluminum to the stable closed-shell $3d^{10}4s^2$ configuration of zinc is demonstrated to lead to a $^2\Pi_r$ ground state in the following article. Despite the commonality of $^2\Pi_r$ ground states in AlCa, AlZn, AlAr, and AlKr, the high vibrational frequencies in AlCa (189 cm^{-1}) and AlZn ($\Delta G_{1/2}$=153.4 cm^{-1}) (Ref. 3) as compared to AlAr (31.6 cm^{-1}) (Ref. 15) and AlKr (39.0 cm^{-1}) (Ref. 15) are indicative of significant chemical bonding in the intermetallic molecules; such effects are absent in the complexes of aluminum with a rare gas due to the severe mismatch in orbital energies between the constituent atoms.

The rotational analysis of eight vibronic bands has allowed the ground state of AlCa to be assigned as $X\ ^2\Pi_r$, and a weighted least squares analysis of the measured rotational constants provides a ground state bond length of $r_0(X\ ^2\Pi_r)=3.1479\pm0.0010$ Å, in marked contrast to the bond lengths of AlCu (2.3389±0.0004 Å) (Ref. 1) and AlNi (2.3211±0.0007 Å).[2] The observation of four assignable band systems has led to the identification of four excited electronic states in AlCa; the [13.5] $^2\Pi_r$ state, the [15.8] $^2\Sigma$ state, the [17.0] $^2\Delta$ (?) state, and the [17.6] $^2\Delta_{3/2}$ state.

The potential energy curves of seven low-lying electronic states of AlCa and the ground $^1\Sigma^+$ state of $AlCa^+$ have been computationally investigated using two sophisticated *ab initio* techniques. In agreement with experimental results, the $^2\Pi_r$ state is calculated to be the ground state for neutral AlCa and is predicted to be bound by 0.47 eV with respect to dissociation into $Al(^2P^0)+Ca(^1S)$. A $^2\Sigma^+$ state is predicted to be the lowest excited state of AlCa, and molecular parameters for this state and five other low-lying excited electronic states [$^4\Sigma^-$, $^4\Pi_r$, $^2\Pi_r(2)$, $^2\Delta$, and $^2\Sigma^-$] have been computed. The $AlCa^+$ cation is found to have a $^1\Sigma^+$ ground electronic state with a dissociation energy to $Al^+(^1S)+Ca(^1S)$ of 1.50 eV. The calculated vertical (5.03 eV) and adiabatic (4.97 eV) ionization energies of AlCa agree well with the experimental ionization energy of 5.072±0.028 eV.

ACKNOWLEDGMENTS

We thank Michael A. Weibel and Caleb A. Arrington for their time and expertise in preparing the AlCa alloys used, and thank Professor William H. Breckenridge for the use of the intracavity étalon employed in some of the high resolution studies. Research support from NSF under Grant Nos. 5. CHE-9215193 to M.D.M. and CHE-9116286 to J.S. is gratefully acknowledged. J.M.B. heartily thanks the Eastman Kodak Company for a predoctoral fellowship, and acknowledgment is also made to the donors of the Petroleum Research Fund, administered by the American Chemical Society, for partial support of this research.

[1] J. M. Behm, C. A. Arrington, J. D. Langenberg, and M. D. Morse, J. Chem. Phys. **99**, 6394 (1993).
[2] J. M. Behm, C. A. Arrington, and M. D. Morse, J. Chem. Phys. **99**, 6409 (1993).
[3] J. M. Behm, T. Blume, and M. D. Morse, J. Chem. Phys. **101**, 5454 (1994).
[4] C. E. Moore, Natl. Bur. Stand. (U.S.) Circ. 467 (1949, 1952, 1971).
[5] Z.-W. Fu, G. W. Lemire, Y. Hamrick, S. Taylor, J.-C. Shui, and M. D. Morse, J. Chem. Phys. **88**, 3524 (1988).
[6] S. C. O'Brien, Y. Liu, Q. Zhang, J. R. Heath, F. K. Tittel, R. F. Curl, and R. E. Smalley, J. Chem. Phys. **84**, 4074 (1986).
[7] S. Gerstenkorn and P. Luc, *Atlas du Spectre d'Absorption de la Molécule d'Iode: 14800–20000 cm^{-1}* (CNRS, Paris, 1978); Rev. Phys. Appl. **14**, 791 (1979).
[8] S. Gerstenkorn and P. Luc, *Atlas du Spectre d'Absorption de la Molécule d'Iode: 14000–15600 cm^{-1}* (CNRS, Paris, 1978).
[9] D. J. Clouthier and J. Karolczak, Rev. Sci. Instrum. **61**, 1607 (1990).
[10] P. R. Bevington, *Data Reduction and Error Analysis for the Physical Sciences* (McGraw–Hill, New York, 1969), CURFIT program, pp. 235–245.
[11] See AIP document No. PAPS JCPSA-101-5441-3 for 3 pages of absolute line positions. Order by PAPS number and journal reference from American Institute of Physics, Physics Auxiliary Publication Service, Carolyn Gehlbach, 500 Sunnyside Boulevard., Woodbury, New York 11797-2999. The price is $1.50 for each microfiche (98 pages) or $5.00 for photocopies of up to 30 pages, and $0.15 for each additional page over 30 pages. Airmail additional. Make checks payable to the American Institute of Physics.
[12] G. Herzberg, *Molecular Spectra and Molecular Structure I. Spectra of Diatomic Molecules* (Van Nostrand Reinhold, New York, 1950), pp. 220–228.
[13] H. Lefebvre-Brion and R. W. Field, *Perturbations in the Spectra of Diatomic Molecules* (Academic, Orlando, 1986).
[14] S. A. Heidecke, Z.-W. Fu, J. R. Colt, and M. D. Morse, J. Chem. Phys. **97**, 1692 (1992).
[15] C. L. Callender, S. A. Mitchell, and P. A. Hackett, J. Chem. Phys. **90**, 5252 (1989).
[16] B. O. Roos, in *Ab Initio Methods in Quantum Chemistry, Part II*, Adv. Chem. Phys., edited by K. P. Lawley (Wiley, Chichester, 1987), Vol. 69; P.-Å. Malmqvist, A. Rendell, and B. O. Roos, J. Phys. Chem. **94**, 5477 (1990).
[17] E. R. Davidson, in *The World of Quantum Chemistry*, edited by R. Daudel (Reidel, Dortrecht, 1974), p. 17; S. R. Langhoff and E. R. Davidson, Int. J. Quantum Chem. **8**, 61 (1974).
[18] P.-O. Widmark, B. J. Persson, and B. O. Roos, Theor. Chim. Acta **79**, 419 (1991).
[19] A. J. Sadlej, Theor. Chim. Acta **79**, 123 (1991).
[20] K. Anderson, M. P. Fulscher, R. Lindh, P.-Å. Malmqvist, J. Olsen, B. O. Roos, and A. Sadlej, University of Lund, Sweden and P.-O. Widmark, IBM, Sweden, MOLCAS-2.
[21] J. A. Pople, M. Head-Gordon, and K. Raghavachari, J. Chem. Phys. **87**, 5968 (1987).
[22] A. Schäfer, H. Horn, and R. Ahlrichs. J. Chem. Phys. **97**, 2571 (1992).
[23] M. J. Frisch, G. W. Trucks, M. Head-Gordon, P. M. W. Gill, M. W. Wong, J. B. Foresman, B. G. Johnson, H. B. Schlegel, M. A. Robb, E. S. Replogle, R. Gomperts, J. L. Anders, K. Raghavachari, J. S. Binkley, C. Gonzales, R. L. Martin, D. J. Fox, D. J. DeFrees, J. Baker, J. J. P. Stewart, and J. A. Pople, GAUSSIAN 92, Revision C, Gaussian Inc., Pittsburgh, Pennsylvania, 1992.
[24] C. W. Bauschlicher, Jr., S. R. Langhoff, and H. Partridge, J. Chem. Phys. **84**, 901 (1986).